

Electronic supplementary information

of

New Tetridentate N,O-Hybrid Phenanthroline-Derived Organophosphorus Extractants for the Separation and Complexation of Trivalent Actinides and Lanthanides

Xiao Yang[†], Shihui Wang[†], Lei Xu[§], Qiang Yan[‡], Chao Xu[‡], Petr Matveev[#], Lecheng
Lei[†], Chengliang Xiao^{†*}

[†]College of Chemical and Biological Engineering, Zhejiang University, Hangzhou 310027, China

[‡]Institute of Nuclear and New Energy Technology, Tsinghua University, Beijing 100084, China

[§]Institute of Nuclear-Agricultural Science, Zhejiang University, Hangzhou 310058, China

[#]Radiochemistry Division, Department of Chemistry, Lomonosov Moscow State University,
Moscow 119991, Russian Federation

*Email: xiaoc@zju.edu.cn (Chengliang Xiao)

Contents

1. $^1\text{H}/^{31}\text{P}$ NMR spectra and Maldi-Tof MS of ligands	Page S2-S3
2. ^{31}P NMR titration spectra and peak positions of ^1H NMR spectra	Page S4-S5
3. UV-vis spectra titrated with $\text{La}(\text{NO}_3)_3$ and $\text{Lu}(\text{NO}_3)_3$	Page S6-S8
4. Structure of $\text{Lu}(\text{L}_1)(\text{NO}_3)_3$	Page S9
5. Crystal data and structure refinement	Page S10-S11
6. Main bond distances and angles	Page S12-

¹H/³¹P NMR spectra and Maldi-Tof MS of ligands.

¹H NMR

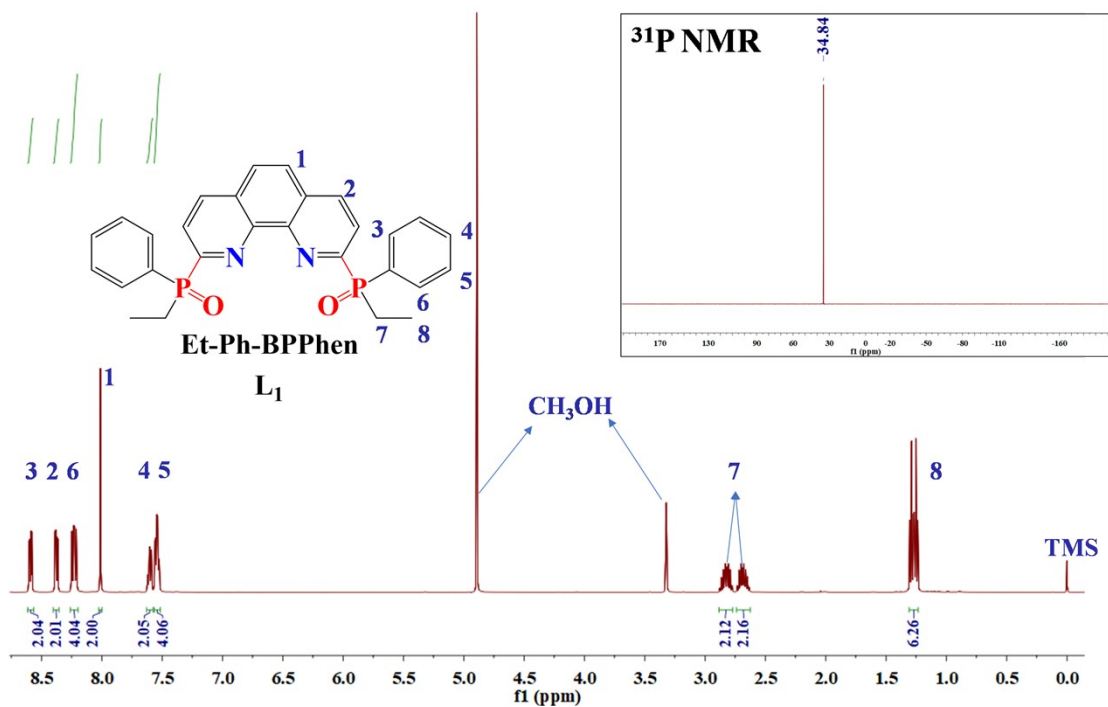


Figure S1. ¹H NMR of Et-Ph-BPPhen (\mathbf{L}_1).

MALDI-TOF Mass Spectrum

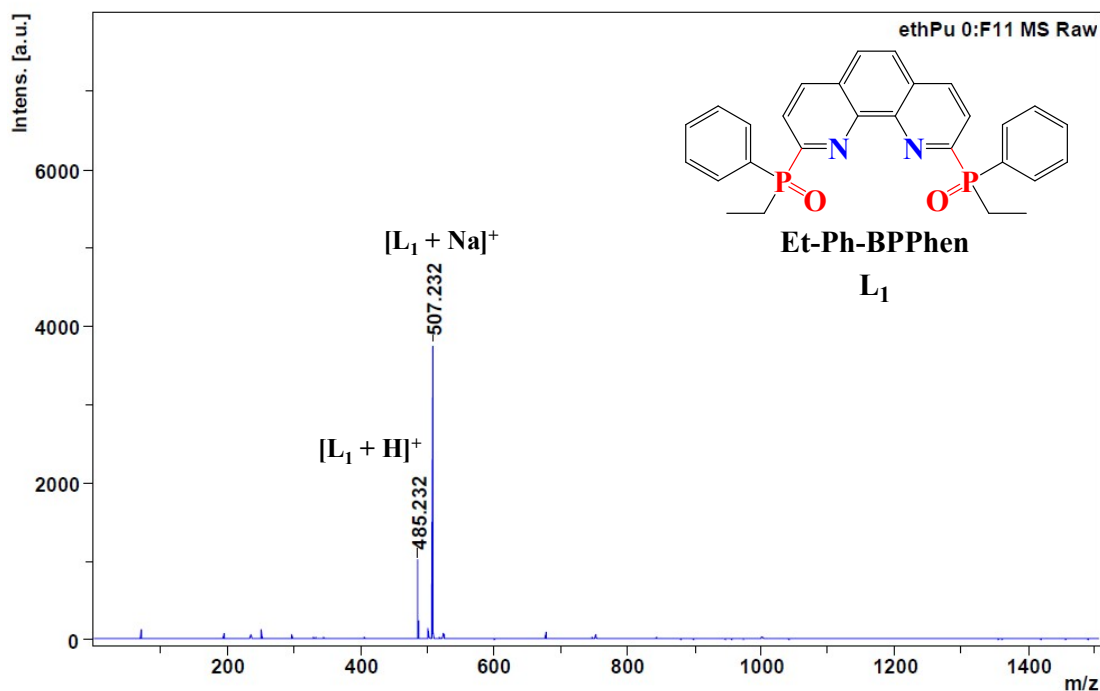


Figure S2. Maldi-Tof MS of Et-Ph-BPPhen (L_1).

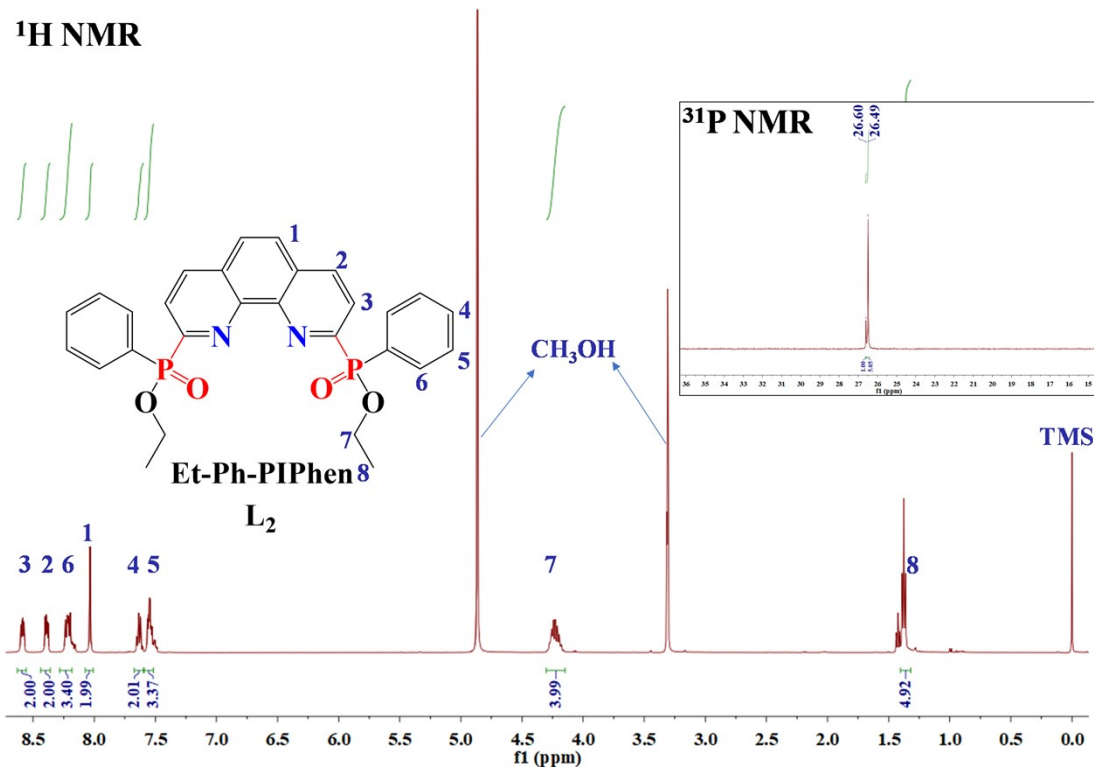


Figure S3. ^1H and ^{31}P NMR of Et-Ph-PIPhen (L_2).

MALDI-TOF Mass Spectrum

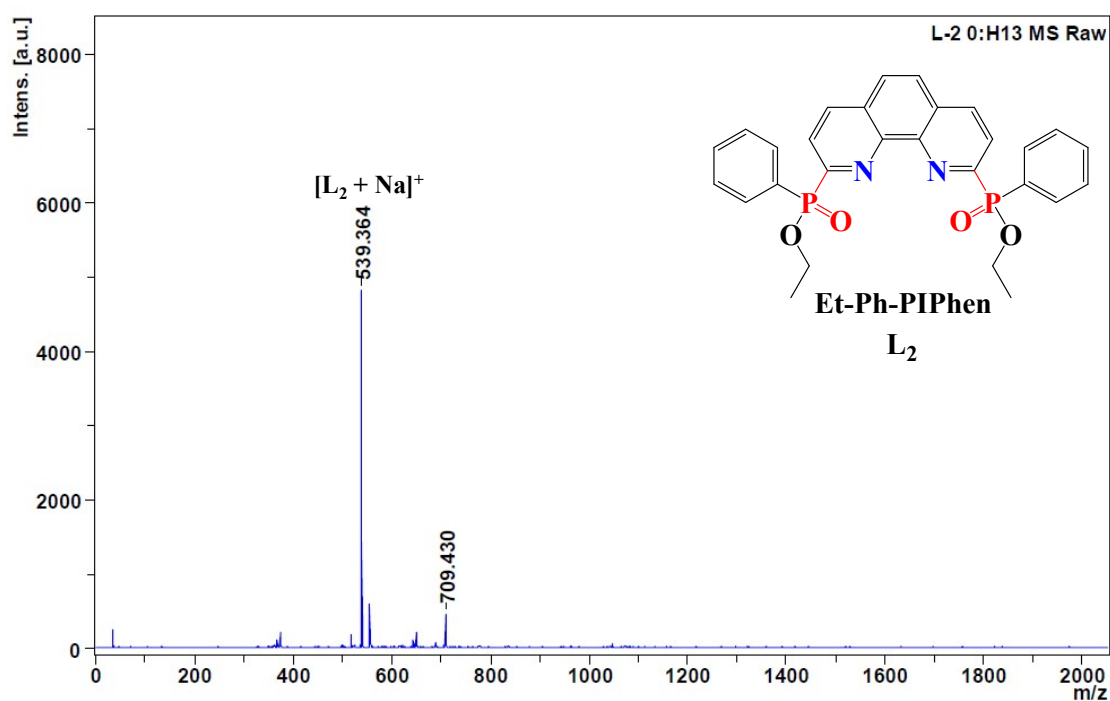


Figure S4. Maldi-Tof MS of Et-Ph-PIPhen (L_2).

^{31}P NMR titration spectra and peak positions of 1H NMR spectra.

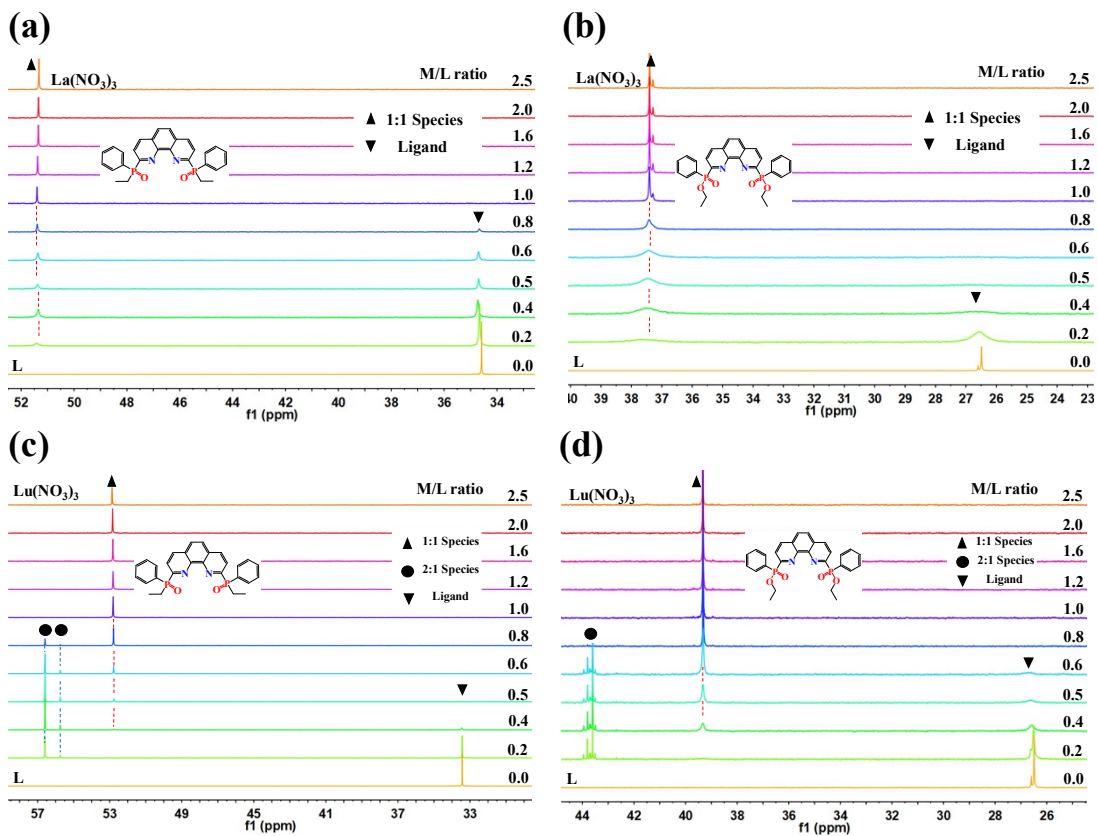


Figure S5. (a) ^{31}P NMR spectra of \mathbf{L}_1 (10.0 mM) titrated with $\text{La}(\text{NO}_3)_3$ (0 - 2.5 equiv.) in CD_3OD ; (b) ^{31}P NMR spectra of \mathbf{L}_2 (10.0 mM) titrated with $\text{La}(\text{NO}_3)_3$ (0 - 2.5 equiv.) in CD_3OD ; (c) ^{31}P NMR spectra of \mathbf{L}_1 (10.0 mM) titrated with $\text{Lu}(\text{NO}_3)_3$ (0 - 2.5 equiv.) in CD_3OD ; (d) ^{31}P NMR spectra of \mathbf{L}_2 (10.0 mM) titrated with $\text{Lu}(\text{NO}_3)_3$ (0 - 2.5 equiv.) in CD_3OD . M/L denotes the metal/ligand equivalents.

Table S1 The peak positions of ligands and complexes in ^1H NMR spectra

Systems	Figures	0:1	M/L ratio		
			1:1	1:2	
La(III)-to- L₁	4a	8.56, 8.42, 8.25, 8.03, 7.58 and 7.51 ppm	8.77, 8.23, 8.20, 8.10, 7.73 and 7.67 ppm	-	
			8.76, 8.23, 8.20, 8.10, 7.73 and 7.68 ppm	-	
Lu(III)-to- L₁	4b	8.59, 8.39, 8.22, 8.03, 7.63 and 7.55 ppm	9.01, 8.54, 8.36, 8.14, 7.78 and 7.70 ppm	9.42, 9.38, 9.08, 8.69, 7.44, 7.35, 7.24 and 7.09 ppm	
			9.03, 8.53, 8.38, 8.19, 7.83 and 7.71 ppm	9.06-9.55, 8.66 and 6.98-7.78 ppm	
Lu(III)-to- L₂	4d	8.59, 8.39, 8.22, 8.03, 7.63 and 7.55 ppm			

UV-vis spectra titrated with La(NO₃)₃ and Lu(NO₃)₃.

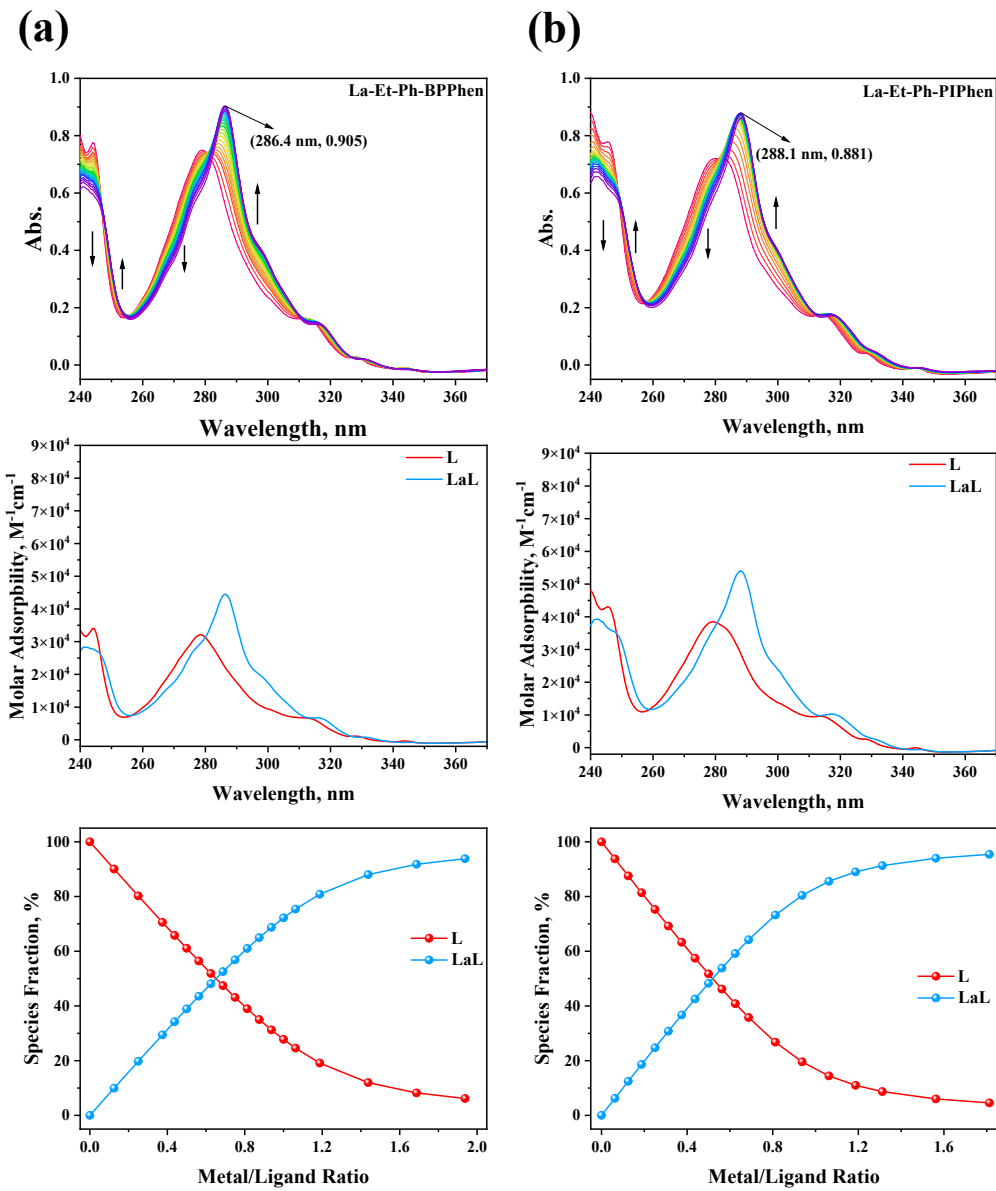


Figure S6. Spectra of ligands (\mathbf{L}_1 and \mathbf{L}_2) titrated with La(NO₃)₃ in methanol solution (T = 298 K, I = 0.01 M Et₄NNO₃, V₀ = 2.00 mL). (a) Top: the normalized absorption spectra of \mathbf{L}_1 varied with the La(NO₃)₃ concentration; Middle: the fitted molar absorptivity of the ligand and La(III) complexes; Bottom: the species fraction curves obtained during the titration process. C_L = 0.023 mM, C_{La(III)} = 0.24 mM, 0.31 mL titrant was added totally. (b) Top: the normalized absorption spectra of \mathbf{L}_2 varied with the La(NO₃)₃ concentration; Middle: the fitted molar absorptivity of the

ligand and La(III) complexes; Bottom: the species fraction curves obtained during the titration

process. $C_L = 0.019 \text{ mM}$, $C_{\text{La(III)}} = 0.24 \text{ mM}$, 0.29 mL titrant was added totally.

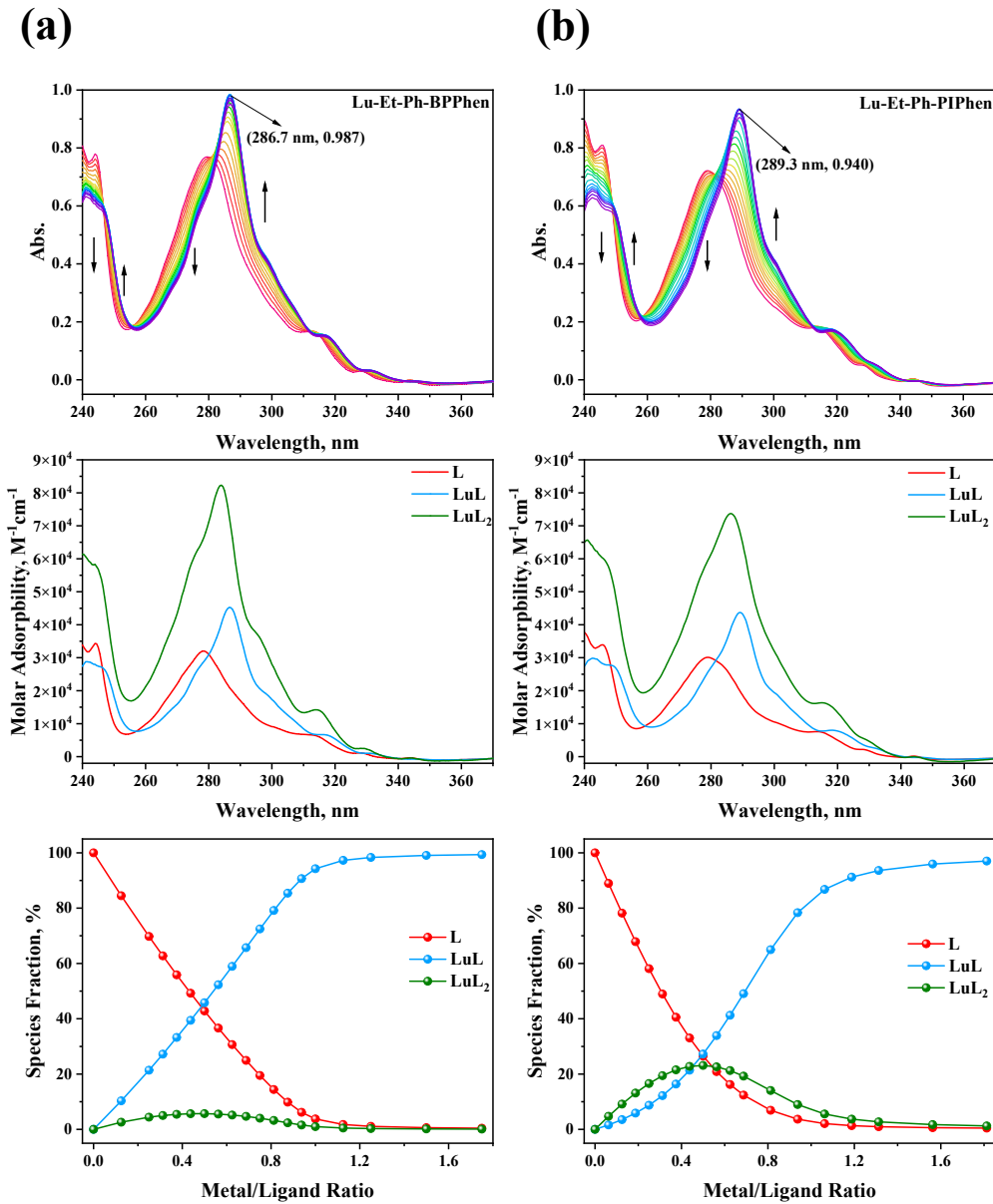


Figure S7. Spectra of ligands (\mathbf{L}_1 and \mathbf{L}_2) titrated with $\text{Lu}(\text{NO}_3)_3$ in methanol solution ($T = 298 \text{ K}$, $I = 0.01 \text{ M Et}_4\text{NNO}_3$, $V_0 = 2.00 \text{ mL}$). (a) Top: the normalized absorption spectra of \mathbf{L}_1 varied with the $\text{Lu}(\text{NO}_3)_3$ concentration; Middle: the fitted molar absorptivity of the ligand and Lu(III) complexes; Bottom: the species fraction curves obtained during the titration process. $C_L = 0.024$

mM, $C_{\text{Lu(III)}} = 0.30$ mM, 0.31 mL titrant was added totally. (b) Top: the normalized absorption spectra of \mathbf{L}_2 varied with the $\text{Lu}(\text{NO}_3)_3$ concentration; Middle: the fitted molar absorptivity of the ligand and Lu(III) complexes; Bottom: the species fraction curves obtained during the titration process. $C_L = 0.024$ mM, $C_{\text{Lu(III)}} = 0.30$ mM, 0.31 mL titrant was added totally. $C_L = 0.024$ mM, $C_{\text{Lu(III)}} = 0.30$ mM, 0.29 mL titrant was added totally.

Structure of Lu(L₁)(NO₃)₃.

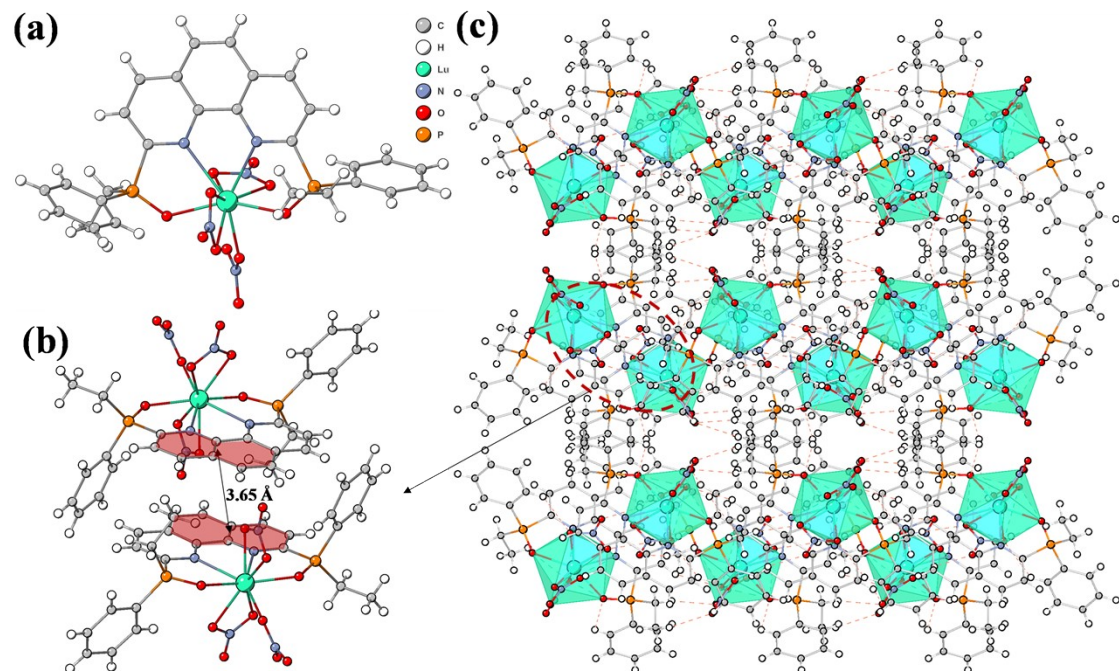


Figure S8. (a) Crystal structure, (b) π - π stacking interaction and (c) crystal packing of Lu(L₁)(NO₃)₃ viewed along with a-axis. Hydrogen bonds are presented by red dashed lines. The solvent molecules have been omitted for clarity. The Lu, O, N, P, C and H atoms are represented by light cyan, red, pastel blue, orange, light grey, and white colours, respectively.

Crystal data and structure refinement.

Table S2. Crystal data and structure refinement for the crystals related to \mathbf{L}_1 .

	La(\mathbf{L}_1)(NO ₃) ₃	Eu(\mathbf{L}_1)(NO ₃) ₃	Lu(\mathbf{L}_1)(NO ₃) ₃
CCDC	2112088	2112094	2112093
Empirical formula	C ₂₈ H ₂₆ LaN ₅ O ₁₁ P ₂	C ₂₈ H ₂₆ EuN ₅ O ₁₁ P ₂	C ₂₈ H ₂₆ LuN ₅ O ₁₁ P ₂
Formula weight	809.39	822.44	845.45
Temperature/K	170	170	170
Crystal system	orthorhombic	orthorhombic	orthorhombic
Space group	Pbca	Pbca	Pbca
a/ \AA	17.6729(5)	17.6662(5)	17.275(8)
b/ \AA	17.7777(5)	17.5454(5)	17.814(8)
c/ \AA	20.2305(6)	20.1869(6)	20.383(9)
$\alpha/^\circ$	90	90	90
$\beta/^\circ$	90	90	90
$\gamma/^\circ$	90	90	90
Volume/ \AA^3	6356.1(3)	6257.1(3)	6273(5)
Z	8	8	8
ρ_{calc} g/cm ³	1.692	1.746	1.79
μ/mm^{-1}	1.512	2.175	3.318
F(000)	3232	3280	3344
Crystal size/mm ³	0.12 × 0.1 × 0.02	0.25 × 0.13 × 0.1	0.04 × 0.02 × 0.02
Radiation	MoK α ($\lambda = 0.71073$)	MoK α ($\lambda = 0.71073$)	MoK α ($\lambda = 0.71073$)
2 θ range for data collection/°	3.822 to 60.078	3.844 to 72.202	4.572 to 55.598
Index ranges	-24 ≤ h ≤ 20, -25 ≤ k ≤ 25, -28 ≤ l ≤ 28	-29 ≤ h ≤ 24, -27 ≤ k ≤ 26, -32 ≤ l ≤ 32	-22 ≤ h ≤ 22, -22 ≤ k ≤ 22, -25 ≤ l ≤ 23
Reflections collected	131263	169270	47883
Independent reflections	9295 [R _{int} = 0.0687, R _{sigma} = 0.0270]	13957 [R _{int} = 0.0411, R _{sigma} = 0.0254]	6809 [R _{int} = 0.0768, R _{sigma} = 0.0471]
Data/restraints/parameters	9295/0/426	13957/0/426	6809/0/426
Goodness-of-fit on F ²	1.043	1.031	1.04
Final R indexes [I >= 2σ (I)]	R ₁ = 0.0289, wR ₂ = 0.0596	R ₁ = 0.0257, wR ₂ = 0.0489	R ₁ = 0.0364, wR ₂ = 0.0750
Final R indexes [all data]	R ₁ = 0.0422, wR ₂ = 0.0662	R ₁ = 0.0439, wR ₂ = 0.0537	R ₁ = 0.0580, wR ₂ = 0.0850
Largest diff. peak/hole/e \AA^{-3}	0.43/-0.76	0.59/-0.95	1.57/-0.92

Table S3. Crystal data and structure refinement for the crystals related to **L₂**.

	(La) ₂ (L ₂) ₂ (NO ₃) ₆ ·CH ₃ OH	Eu(L ₂)(NO ₃) ₃
CCDC	2112095	2124871
Empirical formula	C ₅₈ H ₆₀ La ₂ N ₁₀ O ₂₈ P ₄	C ₂₈ H ₂₆ EuN ₅ O ₁₃ P ₂
Formula weight	1746.86	854.44
Temperature/K	170	170
Crystal system	monoclinic	orthorhombic
Space group	P2 ₁ /c	Pna21
a/Å	16.500(6)	16.516(5)
b/Å	25.533(7)	14.612(5)
c/Å	17.385(9)	13.254(4)
α/°	90	90
β/°	95.61(2)	90
γ/°	90	90
Volume/Å ³	7289(5)	3198.5(17)
Z	4	4
ρ _{calc} g/cm ³	1.592	1.774
μ/mm ⁻¹	1.331	2.136
F(000)	3504	1704
Crystal size/mm ³	0.39 × 0.26 × 0.16	0.09 × 0.03 × 0.02
Radiation	MoKα (λ = 0.71073)	MoKα (λ = 0.71073)
2θ range for data collection/°	3.922 to 61.088	4.826 to 54.336
Index ranges	-23 ≤ h ≤ 23, -36 ≤ k ≤ 34, -24 ≤ l ≤ 24	-21 ≤ h ≤ 21, -18 ≤ k ≤ 18, -17 ≤ l ≤ 17
Reflections collected	146615	105406
Independent reflections	22284 [R _{int} = 0.0564, R _{sigma} = 0.0382]	7094 [R _{int} = 0.0610, R _{sigma} = 0.0244]
Data/restraints/parameters	22284/167/997	7094/1/444
Goodness-of-fit on F ²	1.03	1.054
Final R indexes [I >= 2σ (I)]	R ₁ = 0.0440, wR ₂ = 0.1034	R ₁ = 0.0308, wR ₂ = 0.0788
Final R indexes [all data]	R ₁ = 0.0724, wR ₂ = 0.1179	R ₁ = 0.0342, wR ₂ = 0.0814
Largest diff. peak/hole/e Å ⁻³	1.61/-1.19	1.31/-0.85

Main bond distances and angles.

Table S4. Main bond distances and angles for the La(**L**₁)(NO₃)₃ complex.

Bond/Angle	Å/°
La-O1	2.4357(15)
La-O2	2.4852(15)
La-O3	2.5925(17)
La-O4	2.5988(19)
La-O6	2.6770(18)
La-O7	2.5941(16)
La-O9	2.6259(17)
La-O10	2.6029(17)
La-N1	2.7947(17)
La-N2	2.7722(18)
O1-La-O2	158.69(5)

Table S5. Main bond distances and angles for the Eu(**L**₁)(NO₃)₃ complex.

Bond/Angle	Å/°
Eu-O1	2.3465(11)
Eu-O2	2.3971(10)
Eu-O3	2.4973(11)
Eu-O4	2.4952(12)
Eu-O6	2.6569(13)
Eu-O7	2.4869(11)
Eu-O9	2.5415(12)
Eu-O10	2.4921(11)
Eu-N1	2.7150(11)
Eu-N2	2.6844(12)
O1-Eu-O2	155.41(4)

Table S6. Main bond distances and angles for the Lu(**L**₁)(NO₃)₃ complex.

Bond/Angle	Å/°
Lu-O1	2.372(3)
Lu-O2	2.301(3)
Lu-O3	2.370(4)
Lu-O4	2.421(4)
Lu-O6	2.270(3)
Lu-O9	2.482(4)
Lu-O10	2.314(3)
Lu-N1	2.551(4)
Lu-N2	2.639(4)
O1-Lu-O2	152.29(12)

Table S7. Main bond distances and angles for the (La)₂(**L**₂)₂(NO₃)₆·CH₃OH complex.

Bond/Angle	Å/°	Bond/Angle	Å/°
La1-O1	2.516(2)	La2-O15	2.469(3)
La1-O3	2.523(2)	La2-O17	2.482(2)
La1-O5	2.730(3)	La2-O22	2.678(3)
La1-O6	2.612(3)	La2-O23	2.586(3)
La1-O8	2.628(3)	La2-O25	2.620(5)
La1-O9	2.705(3)	La2-O26	2.628(4)
La1-O11	2.743(3)	La2-O19	2.531(14)
La1-O12	2.640(3)	La2-O19A	2.553(5)
La1-O14	2.550(3)	La2-O21A	2.575(4)
La1-N1	2.787(3)	La2-N6	2.774(2)
La1-N2	2.790(3)	La2-N7	2.768(3)
O1-La1-O3	168.71(7)	O15-La2-O17	149.49(10)

Table S8. Main bond distances and angles for the Eu(**L**₂)(NO₃)₃ complex.

Bond/Angle	Å/°
Eu1-O1	2.355(4)
Eu1-O3	2.361(4)
Eu1-O5	2.539(5)
Eu1-O6	2.498(6)
Eu1-O8	2.496(6)
Eu1-O9	2.567(9)
Eu1-O11	2.513(5)
Eu1-O12	2.468(5)
Eu1-N1	2.672(6)
Eu1-N2	2.668(5)
O1-La1-O3	154.29(15)